

SEISMIC VULNERABILITY ASSESSMENT OF AN HISTORICAL UNREINFORCED MASONRY BUILDING OF THE XIXTH CENTURY: EL FETH HIGH SCHOOL IN BLIDA, ALGERIA

Abderrahmen Souleymen HENNI CHEBRA^{*}, Mustapha CHEIKH-ZOUAOU¹,
Amina ABDESSEMED-FOUFA¹

¹ University of Blida 1. Lab ETAP "Environment and Technology for Architecture and Cultural Heritage, Institute of Architecture and Urban Planning (I.A.U), Blida, (09000), Algeria.

Abstract

Schools in Algeria, built in the XIXth and XXth centuries, are not only places of education and learning, but make up a rich cultural heritage of architectural techniques and traditional know-how. However, their seismic vulnerability risks the safety of their occupants. They were built of masonry before seismic regulations were put into place, which increases their sensitivity to seismic hazard. Algeria is situated in a well-known zone of high seismic activity and the risk to these buildings challenges their structural behaviour. This study focuses on an assessment of seismic vulnerability on a specimen built entirely in hollow brick which wonderfully represents this architectural heritage leading to a better understanding of the potential risks for these buildings, at a structural level. Macro element models, using the Tremuri software, are subjected to a non-linear "Pushover" analysis in order to determine the degree of vulnerability and locate the weak sections of the structure which could collapse during seismic action. This study aims to highlight the seismic risks of these types of structures and also offer appropriate guidelines and recommendations that could be of use during a possible rehabilitation or conservation program of this built heritage site.

Keywords: School building; 19th century architecture; Unreinforced masonry "URM"; Seismic vulnerability; Macro element; Pushover analysis

Introduction

Seismic vulnerability of existing buildings.

In recent years, many scientific researchers have addressed the question of seismic vulnerability in unreinforced masonry (URM) buildings and have studied their behaviour during an earthquake. Unreinforced masonry (URM) buildings have a tendency to be more susceptible to earthquake damage than other actual forms of construction. However, this is not only due to the fact that they were built with no consideration to seismic shock but also because the masonry is of poor ductility [1].

Before the advent of seismic standards, seismic vulnerability, exacerbated by building concentration, led to a high level of seismic risk, even in areas where seismicity was considered moderate. Consequently, several methods to evaluate seismic vulnerability were established in many countries as part of a greater international program [2].

Ancient masonry buildings, that is to say, those built before seismic regulations were put into place, are generally vulnerable [2, 3]. However, there are monumental constructions, well-built according to the right know-how and with quality materials, which withstand seismic

^{*} Corresponding author: soul_archi@live.com

shock. On the other hand, other apparently similar structures damage very easily: an analysis of their vulnerability consists, therefore, in not only trying to predict their behaviour during an earthquake, by integrating all the elements of uncertainty, but also in detecting any eventual errors in the seismic design [3]. Compared to other construction materials, masonry shows a non-linear behaviour for lower seismic demands. In addition to its low tensile strength [4] its weakness is mainly due to its physical and mechanical characteristics as well as its components (mortar, cement or chaining etc.) [5].

In Algeria, there is a vast colonial building stock dating from the period between 1830 and 1930, built in unreinforced masonry (URM) and without any parasismic design, as was the case for most of the buildings at that time.

North Algeria: a zone of strong seismicity

Throughout history, the north of Algeria has been hit by an important number of earthquakes which caused enormous destructions and heavy loss of human life. Some of the most destructive quakes reached a magnitude of 7.3 on the Richter scale [7]. In northern Algeria, earthquakes predominantly occur at shallow depths, typically within the upper 20 kilometres of the Earth's crust [8].

These earthquakes are mainly produced by reverse or strike-slip faults, driven by the NW-SE to NNW-SSE stress regime resulting from the oblique convergence between the African and Eurasian tectonic plates [8][9]. Even though these earthquakes are shallow, their magnitude and proximity to populated regions can result in substantial damage and fatalities.

According to the Research Center for Astronomy, Astrophysics and Geo-Physics (CRAAG) [7], Algeria has suffered the effects of several earthquakes, some of which were violent and deadly (Table 1). We can cite those of Algiers and Blida in 1716, Oran in 1790, 1825 at Blida, 1867 in Mouzaiaand, Gouraya in 1891. More recent examples include those of Orleansville (09/09/1954), El-Asnam (10/10/1980), Ain Temouchent (22/12/1999), Beni-Ouartilan (10/11/2000) and Bourmedes (21/05/2003). In 2013 and 2018 two recent earthquakes with a magnitude of 5 were felt in the Blida region however no victims or major material damage have been recorded.

Table 1. Some of historical and recent earthquakes in northern Algeria which were felt in Blida. Source: CRAAG

Date	Region	Magnitude	EMS	Deaths	Injuries
1716	Algiers	7.5	X	8000	
1825	Blida	7.5	X-XI	3000	/
1867	Mouzaia	7.5	X-XI		
1891	Gouraya				
1954	Chlef (Ex Orléansville)	6.8	X	1250	3000
1980	Chlef (Ex El Asnam)	7.3	X	5000	9000
1988	Al Affroun	5.4	VII		
1989	Tipasa	6.0	VIII		
2003	Zemmouri	6.8		2278	11450
2013	Blida region	5.1	V	/	/
2018	Blida region	5.4		/	/
2020	Mila	4.9		/	/
2021	Béjaia	6.0		/	04
2022	Oran	5.1		/	/

Blida, a region that has witnessed several earthquakes

Significant seismic events have historically occurred in the Blida region; among the largest in the region's history was the one that hit the town of Blida in 1825; the second was the Mouzaia-El Affroun earthquake of 1867 [10] [11]. The following figure shows the earthquakes that have occurred from 1900 to 2014. We can see the large number of earthquakes that have struck the region over the past century. The Boumerdes earthquake in 2003, used as a reference by the authors of the map, left behind him considerable human and material damage.

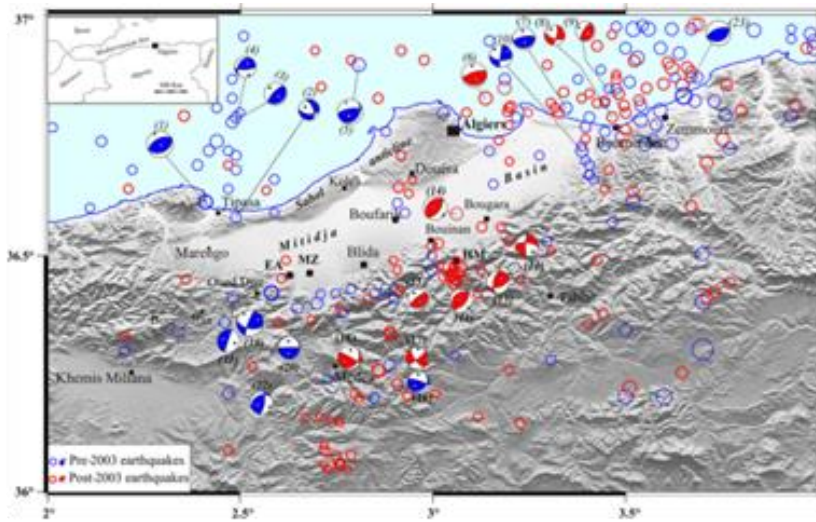


Fig.1. The spatial distribution of earthquakes from 1900 to 2014 (dark, $M \geq 4$: 1900–2003; light, $M \geq 3.5$: 2004–2014), after the continuous recording of Algerian seismic events by Center of Research of Astronomy, Astrophysics and Geophysics.

The urban areas of Blida, particularly its architectural and historical heritage, are highly susceptible to seismic damage, especially older structures made of unreinforced masonry [12].

In the new RPA 2024[13], Algeria is divided into 07 zones of increasing seismicity, ranging from the low seismicity zone (Zone 0) to the high seismicity zone (V & VI) (see Fig 2), where the wilaya of Blida is classified in zone VI, which is high seismicity.

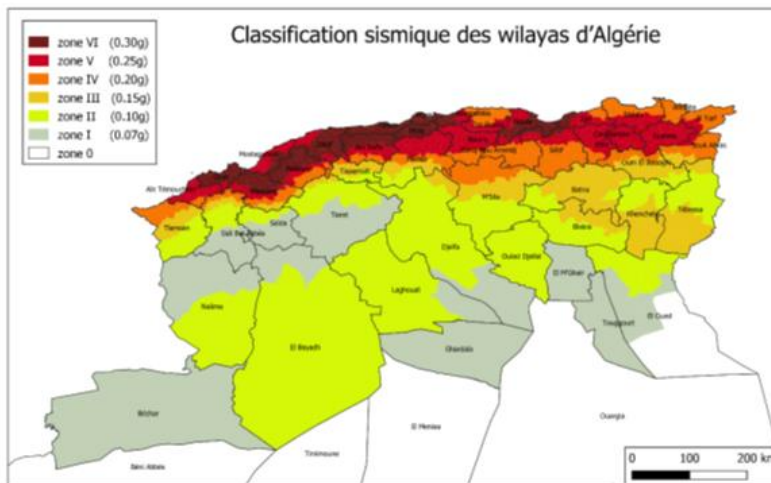

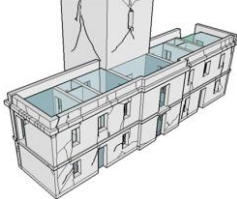




Fig.2. Seismic zoning of Algeria. Source: RPA version 2024[13]

To illustrate the damage that can be caused to unreinforced masonry, research has been carried out on a maritime lighthouse in Boumerdes, 75 km north-east of the town of Blida., Amari [14] et Abdessamed-Foufa [15] conducted an on-site survey to highlight the damage observed on this structure. The following table shows the damages that an unreinforced masonry structure can suffer.

Table 2. Classification of damages and collapse mechanisms. Source: Amari [14] and Abdessemed-Foufa [15].

Damage and deterioration	Description	Illustrations
overturning of the façade	In the vicinity of the corner, the main façade separates from the lateral walls due to the insouciant connection between the orthogonal walls and the floors.	
shear mechanism in-plane	Cracks in the façades: - X-shaped shear cracks - Central vertical crack or arched cracks near the corner - Diagonal cracks (single and crossed) in masonry wall.	
The interior walls' shear cracks.	internal partition walls with both vertical and horizontal fissures.	
Floor damage	A fissure in the vault. Sectional removal of the upper level and separation of the steel IPN beams from the side walls.	

School buildings

A school building is a permanent architectural feature of both the urban and rural landscape. It is one of the most common, and most frequently visited, public buildings in any country. Pertaining to the field of school architecture, it is easily recognizable and becomes, for a pupil, a referent that marks him for life. The history of education in Algeria goes back to well before the French colonial period of 1830 according to *C.E. Chitour* [16]. Teaching was carried out in well-attended Coranic schools, annexed to mosques.

After 1870, the French educational system spread throughout Algeria. Both European and native pupils had, at their disposal, high quality state schools, of every level [16], as well as religious schools. High schools were quickly built in most of the major towns, such as Algiers, Oran, Orléansville and Blida.

With a view to protect a cultural heritage as rich as that of school architecture, composed of places of learning and instruction, which are still in use today, *D.J. Vickery* [17] consider the study of seismic vulnerability is a concept that has significant implications, not only for heritage management, but also for the choice of strategy when faced with seismic.

The safety of school buildings during an earthquake: an indisputable question

Children are some of the most vulnerable people during natural disasters, especially if they are at school when the disaster occurs. In October 2005, more than 16,000 children perished in Pakistan under the rubble of their school buildings when an earthquake struck [18].

According to *G. Kenny* [19], It should be noted that 2,500 children die in the world every year due to the collapse of school buildings. Since 2000, more than 28,000 people in the world have perished in earthquakes because of unsafe school buildings.

D.J. Vickery [17] Remind us that in every society, children represent the future of the nation and schools are places of learning where cultural values and traditional and conventional knowledge are transmitted to the younger generation. If we wish to protect our children from the dangers of natural disasters, besides teaching them what to do when an earthquake occurs, we must protect school buildings by either constructing new anti-seismic establishments or reinforcing schools already in use.

School architecture in Algeria, a heritage to protect:

School architecture bears witness to the importance our society gives to education and youth. Most of the masonry buildings were erected between the XIXth and XXth centuries. These places, consecrated to both life and learning, are inscribed in the history, not only of education, but also of architecture and the nation.

At that time, construction was in unreinforced masonry (URM) using, for the most part, local materials (cut stones, rubble, brick, etc) and buildings were erected with no account given to the seismic factor. Instead, emphasis was put on the artistic style of the period, rather than on the resistance of the building to the horizontal forces that might occur during an earthquake [21].

In 1955, after the earthquake in Orleansville on September 9th, 1954, the first seismic regulations, AS55 [22], were set up. The Algerian regulations, in the form of the 1980 RPA81, were drawn up after the earthquake of El-Asnam on October 10th, 1980. They were revised (RPA 99/2003 version and the RPA 2003 version) after the earthquake of Bourmedes on May 21st, 2003.

During the colonial period, several school buildings were built, ranging from primary schools to secondary and high schools, and adopting architectural expressions pertaining to the great European metropolis, including the neo-classical style, the neo-Moorish style and even eclecticism [20]. These school buildings fall into two distinct categories:

- Establishments built as schools (primary schools; secondary schools; high schools)
- Establishments converted into schools after formerly being used for other functions (barracks; hospital; convent)

After carrying out an inventory in three large towns in the north of Algeria (Algiers, Blida, Oran), we found 105 school buildings (Table 3), made from unreinforced masonry (URM) and dating from 1830 to 1930, officially recognized by the Ministry of National Education. Most were built with no consideration for seismic risk because, at that time, no regulations had been put into place. It is for this reason that the vulnerability and behaviour of these edifices must be evaluated in order to ensure not only their stability but also the safety of their occupants (pupils; teachers; workers).

It is necessary to mention that Table 4 only counts the 14 high schools that we were able to locate and visit, compared to the 18 listed in Table 3.



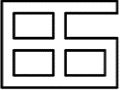
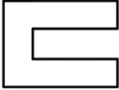
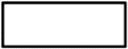

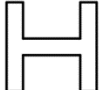

The choice of study case was made in relation to several factors including: (a) its location in an area with high seismicity; (b) the period of its construction between (1830-1930); (c) construction materials and methods " unreinforced masonry (URM) of brick or stone"; (d) complex and unfavorable shape of the building (H – L and U shape) (Table 4), (e) availability of the graphic file and (f) a historical establishment.

Our focus is more on high schools as their occupancy rate is quite high, and as the protection of the occupants comes first, (Table 4) represents the different geometrical shapes encountered when identifying high schools. By taking into account all the parameters of selection, the high school El Feth fulfills all the requirements to carry out our study especially in terms of form not in conformity with the seismic codes and by the important number of daily occupants.

Table 3. Classification, by town and by level, of masonry school buildings.

	Alger	Blida	Oran	Total
Primary school	41	7	19	67
Middle school	8	4	8	20
High school	12	2	4	18

Table 4. High schools inventory classified by geomatic form.

	Geometrical shape	High school
(a)		<u>Rectangular</u> 03
(b)		<u>L-shaped</u> 02
(c)		<u>checkerboard shape</u> 03
(d)		<u>U-shaped</u> 01
(e)		<u>Bar-shaped</u> 02
(f)		<u>Triangular</u> 01
(j)		<u>H-shaped</u> 01
(h)		<u>Irregular shape</u> 01

The aim of our study is to take, as an example, an unreinforced masonry (URM) school building, dating from the period (1830 to 1930), and evaluate the degree of its seismic vulnerability, by using a non-linear static analysis to determine the weakest zones of the structure, with the view of reducing their vulnerability through suitable and reversible repairs, which could be carried out during structural rehabilitation.

Most of these buildings are key infrastructures, classed as category B in the Algerian Seismic Code (RPA99/Ver 2003) [23], and must remain functional during and after an earthquake, in order to meet the demands of the affected population. Reinforcement of these buildings has become, therefore, an absolute priority.

Presentation of the case study: EL Feth highschool (formerly Girls’ Highschool)

El Feth High School (Fig. 3) is situated right in the town centre of Blida, 50km south of the capital, Algiers. The whole establishment has a surface area of 112,700 and 60,000m² of which are covered by buildings. Built as a Christian religious centre and convent in 1865, it was converted, in 1924, into an upper primary school, managed by nuns. During the Second World War, it was used as a trauma centre and during the 1950s; the buildings officially became a high

school named “Girls’ high school”. After Independence in 1962, the Algerian government changed its name to “Lycée El Feth”.



Fig. 3. El Feth High School between the past and the present:
 a - El Feth High School in the present. Source: Design office Bouras;
 b - El Feth High School in the past. Source: www.Blida.net

In 2014, the decision was made to upgrade and partially redevelop the high school, leaving the original structure intact. This project lasted three years.

Architectural and technical description:

The high school, built in the shape of an “H” (Fig. 4), is composed of two storeys and a roof space which stretches over the whole building (Fig. 5). The central building is easily identifiable and it links two almost symmetrical pavilions, punctuated with large evenly-spaced openings. It is of neo-classical style (Fig. 7) and is covered with a red tiled roof.

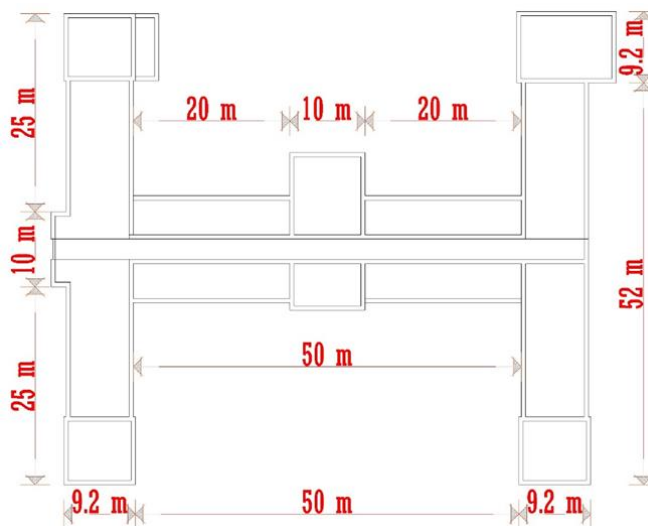


Fig. 4. Plan view of the El Feth High School. Source: Design office Bouras

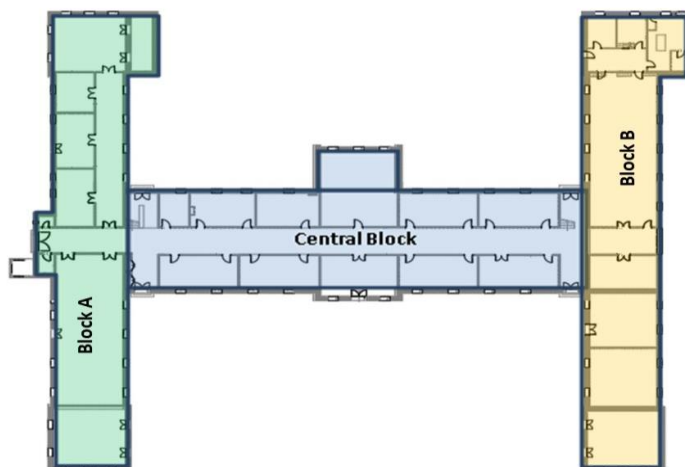


Fig. 5. Description of the plan.

Table 5. Dimensions of the buildings (common floor)

	Block « A »	Central Block	Block « B »
Length (m)	60.00	51.00	60.00
Width (m)	9.20	14.00	9.20
Floor high (m)	4.30	4.30	4.30
Surface (m ²)	552.00	714.00	552.00

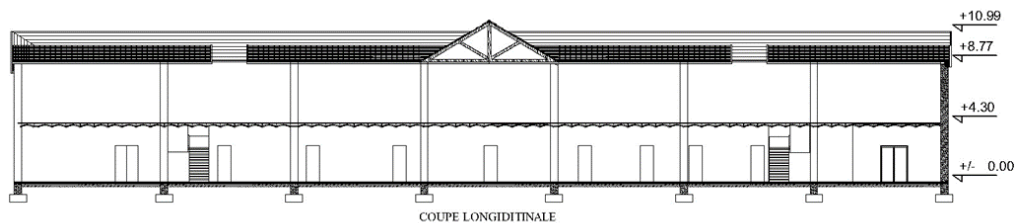


Fig. 6. Longitudinal section of the central block. Source: Design office Bouras

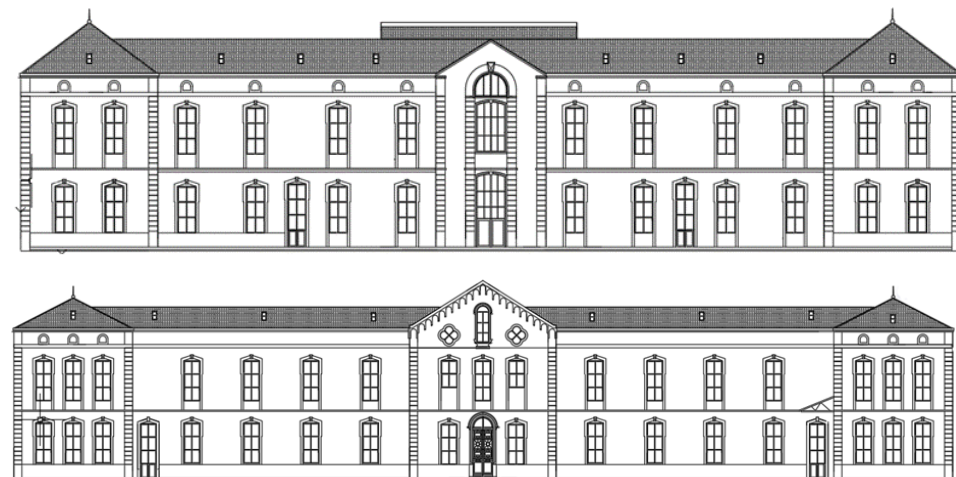


Fig. 7. The two main façade of the High school. Source: Design office Bouras

It is a structure of load-bearing masonry walls, composed of a rubble base and a wall of perforated, baked earth bricks (Fig. 10). There are two different wall thicknesses:

- Facade wall: 55 cm thick (Fig 11)
- Shear wall: 38 cm thick

The ceiling of the first storey is made of a brick vault with metallic beams (see fig 8); the attic ceiling is wooden and is supported by metal profiles.

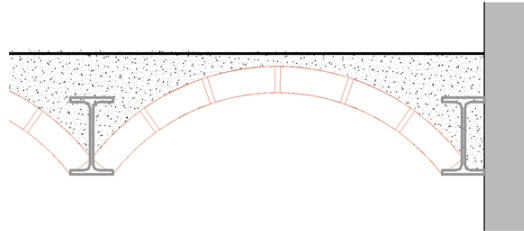


Fig. 8. Detail of vaulted floor. Source: The author

The general shape of the structure is not adequate for seismic behaviour. In addition, the floors, of the 1st and 2nd floor are flexible in their plans; that is to say deformable around the axes OX and OY, therefore do not transmit properly and effectively seismic actions to the bracing elements.



Fig. 9. Perforated, baked earth bricks: a) Secondary load-bearing wall; b) Main load-bearing wall

History of the Brick

The brick industry was controlled by military engineers who imposed stress tests and refused any batches that didn't meet their standards. For restoration purposes, the military sought to improve the brick's resistance to compression by using machines and promoting automation [24]. In the middle of the XVIIIth century, ordinary bricks generally broke under a weight of 35kg. This increased to 50kg half a century later, and to 80kg in 1850. The cost of manufacturing brick also went down, thanks to new elaborate ovens which consumed far less energy than before, during the combustion process.

Hollow Brick with Six Holes

By retracing and relinking these historical facts, the jury of the London World Fair awarded the medal of honour to *M. Borie* [24] for his revolutionary product of the hollow brick. « We have long time needed a material, at the same time solid, light and responsive, which through its shape and the pattern of its solids and voids, can be conveniently and easily joined and overlapped.... » Were, according to *É. Lejeune* [25], the few words of praise expressed by the jury in favour of this new building material. According to *A. Gratry* [26], in the middle of

the XIXth century, France exported large quantities of hollow brick towards its colonies, of which Algeria was one, in order to encourage its production. Thanks to the advent of this material in the field of construction, our case study, El Feth High School, was built using hollow bricks.

Dimensions and brick bond patterns

The dimensions of these bricks vary considerably. However, to make construction easier, builders everywhere make a connection between the three dimensions [24] using a ratio between the length, the width and the thickness (Fig. 10). In our object of study, the El Feth High School, the pattern most commonly found is that of the «Flemish bond». It consists of alternate rows of headers and stretchers (Fig. 8).

Table 6. dimensions of the Borie hollow brick. Source [24]

Designation	Length (cm)	Width (cm)	Thickness (cm)	Dimensions of holes (cm)	Volume including holes (cm ³)
Borie and Co Bricks, 06 holes	22	11	5.5	1.2·1.2	1331

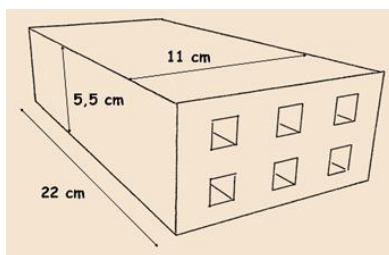


Fig. 10. Shape and dimensions of the hollow brick with 06 holes. Source: author

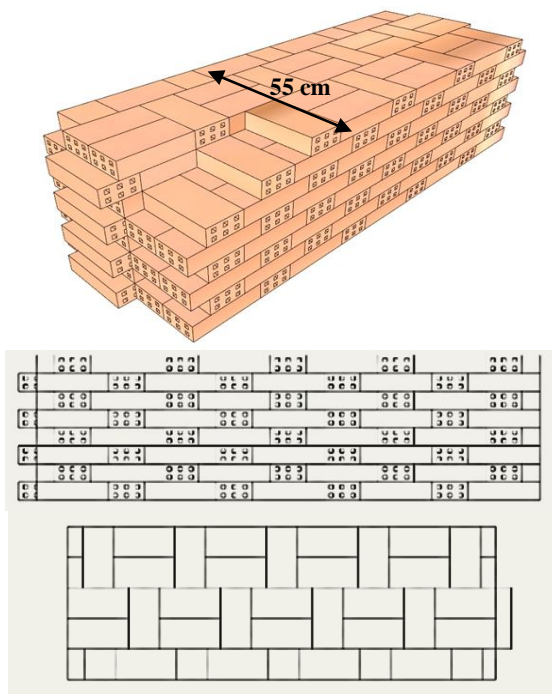


Fig. 11. 55cm thick main load-bearing wall device

It makes the creation of beautiful, decorative motifs possible, with a 10mm joint. In fact, the façades of the high school were, formerly, bare (not covered with mortar) (Fig. 12) and the play between the hollow and filled surfaces could be clearly seen.

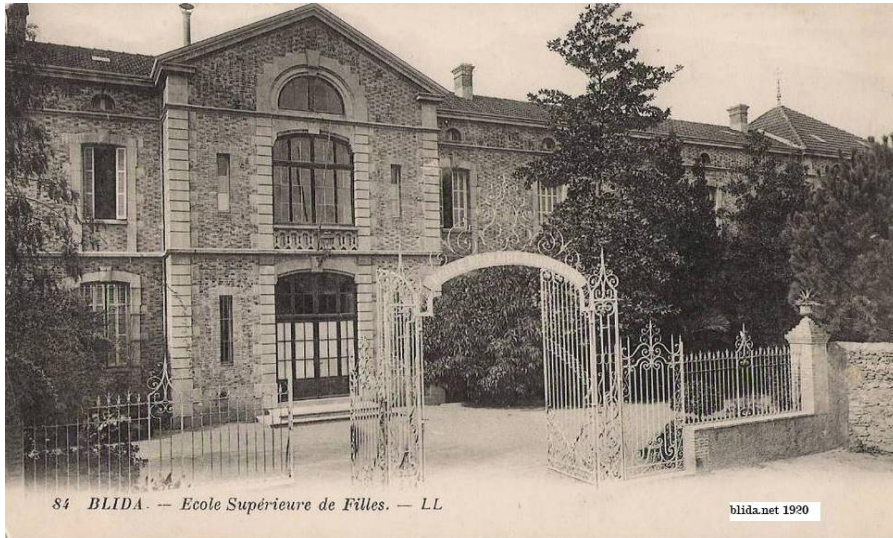


Fig. 12. The main façade without plaster shows the hollow and full faces of bricks on the original construction. Source: www.Blida.net [27]

However, *T. Taguchi and C. Cuadra* [28] Investigated the influence of bond types on the mechanical properties of brick masonry experimentally by compression tests. The researchers came to the conclusion that the lower strength of Flemish bond-type specimens (Fig. 11) was caused by a higher volume of mortar consumption in this bond type. On the other hand, Flemish style bond produces larger volume of vertical bond mortar that crosses the total height of specimens conducting to a failure at lower strength.

The choice of hollow brick as structural material

Thanks to its long sought- after properties of lightness and low cost, hollow brick became more popular than solid brick with the architects and contractors of the XIXth and XXth centuries. Moreover, through its use, a variety of other properties, which couldn't be found to the same extent in solid brick [26], became apparent. These included considerable tensile strength and resistance to atmospheric agents, better connections in the masonry (especially as the mortar penetrates the holes of the brick), greater heat inducibility and complete insulation from moisture.

Methodology

By studying literature related to the evaluation of seismic vulnerability in unreinforced masonry (URM) buildings, several methods and procedures become apparent, ranging from a complex and detailed analysis to a more general perception; the choice of which depended on the amount of information available for the building in question. Our method is based on the basic principles of structural dynamics, a simple and practical procedure, suited, not only to a small budget, but also to a limited level of knowledge about building materials and the state of the connections within this old, unreinforced masonry (URM) building [1].

Modelling by Analogous Frame of Unreinforced Masonry (URM)

The numerous methods set down in literature consider masonry on a different scale [29]. Macro-element modelling seems to be the method that is best suited to the discontinued nature

of masonry [30]. The description of the interaction of its different elements (stone/brick/mortar) through an elastic phase, followed by a softening, gives good results. Non-linear behaviour is successfully reproduced and cracking can be predicted with precision.

The 3MURI method [30] provides simplified formulations of non-linear behaviour of the » macro-elements » model, optimised with precision to carry out non-linear, static analysis of masonry structures. The method, implemented in the software, schematises the structure through an analogous frame made up of macro-elements FME (Frame by Macro-Elements). The distinction between the two different panels (piers and spandrels) is determined by the presence of the openings in the wall.

Macro-elements

The model formulated by *L. Gambarotta and S. Lagomarsino* [31], allows for the study of the non-linear behaviour of masonry walls. Based on the assumption that they have reduced stiffness and deteriorating resistance, it takes into account weaknesses and cracks, resulting in a method that has proved itself to be highly effective in carrying out non-linear, static analysis and testing of cyclic loading.

The construction of an analogous frame

Theoretical and experimental research led to an assimilation of the behaviour of the elements (posts and beams) through a system of equivalent elements. By linking these elements, we obtained a design of an analogous frame, which clearly shows the behaviour of these masonry structures.

Figure 13 shows the basic steps in the idealization of the analogous frame of a masonry wall, marked by a regular distribution of openings: from the identification of posts and beams to that of the rigid zones.

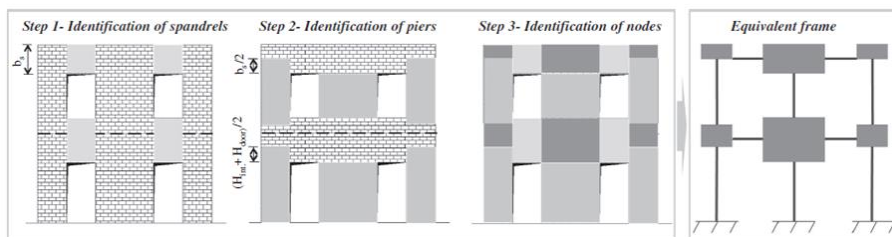


Fig.13. Idealized image of analogous frames in the case of evenly distributed openings. Source: [30].

Modelling of the building using Tremuri software program:

The modelling work was undertaken (Fig. 14) by using the Tremuri software program [30] (academic licence), developed by the company S.T.A DATA.

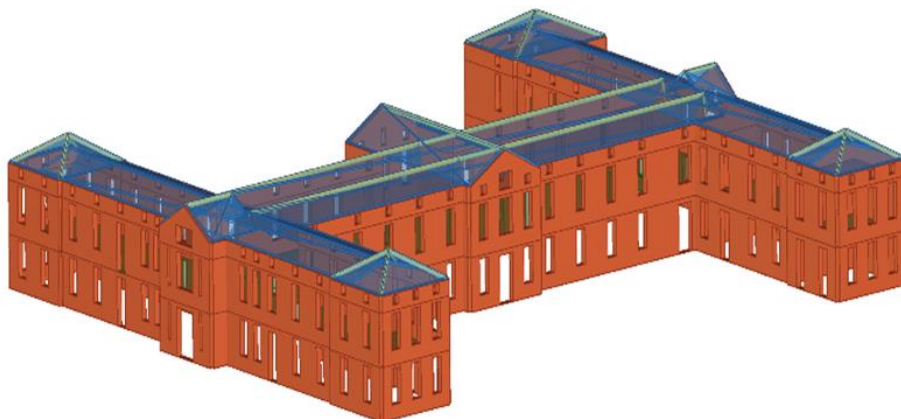


Fig. 14. Modelling of the model from the Tremuri software program

According to Italian standards NTC 2018 (Technical Building Standards) [33], an evaluation of the safety and design of any interventions to be carried out on existing masonry buildings, must take into account the level of knowledge “LC” about the structure. For analysis and verification, standards require the use of confidence factors FC, which modify capacity parameters depending on the level of knowledge linked to geometry, construction details and materials used. The building, with all its components and geometrical forms, is situated in LCI.

The use of the Italian code NTC 2018 fills the gap that is found in all versions of the RPA from 1980 until the last version 2024 [13] about unreinforced masonry [14, 32]; the latter is neither regulated nor authorised in seismic zones. In addition, the TREMURI software has a very diverse library of data relating to the physical and mechanical properties of materials, including perforated bricks; therefore, we've taken the properties closest to the brick in question. So, to perform numerical modelling and analysis, it was necessary to choose the mechanical parameters of the materials from the Italian code NTC 2018 [33].

Recommendations for this level of knowledge stipulate that the values chosen for material properties must be minimal for resistance and average for the elastic modulus with a confidence factor $FC = 1.35$.

Table 7. Parameters adopted for masonry; Source: NTC 2018 [33]

Materials	f_m (N/cm ²)	τ_0 (N/cm ²)	E (N/cm ²)	G (N/cm ²)	W (KN/m ³)
Masonry in bricks and lime mortar	240	6	1500	500	18

With: f_m = average compressive strength of the masonry; τ_0 = shear strength of the masonry; E = average value of elastic modulus; G = average value of the shear modulus; w = average specific weight of the masonry.

The analogous frame model:

The three-dimensional structure of the building is transformed into an analogous frame model of three defined dimensions – Spandrel beams; Piers; Rigid elements – (Figs 15 and 18) by means of the software auto generation function.

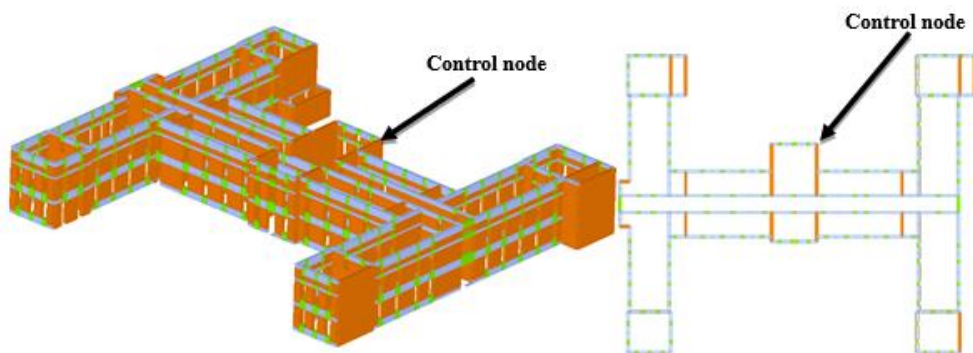


Fig. 15. 3D model created by 3Muri [30]

The numerical model is composed of three types of macro-elements: pier elements, spandrel elements and rigid nodes (858 elements, 816 rigid nodes, that are rigid elements connecting the resisting elements “pier” and “spandrels”).

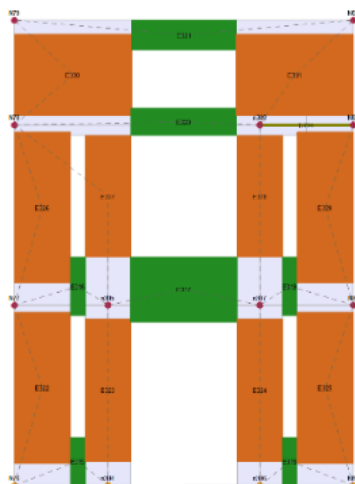


Fig. 16. Analogous frame of the load-bearing wall at the main entrance

In this paper, the spectrum response was calculated following the Algerian seismic code RPA 2003 [14], the 2008 version using equation (1). The spectrum response (Fig. 17) is determined based on the following concepts:

The seismic zone’s classification (the most unfavourable zone III), which is still the same in the new RPA 2024 (zone of high seismicity), then the type of soil must be defined (solid soil S3). The last two elements define the building's usage. (1b: building of great importance) and the constructive components (unreinforced masonry with perforated bricks).

The RPA 2003 [14] defines the response spectrum as the maximum acceleration response curve (S_a/g) of a single-degree-of-freedom system subjected to a particular excitation for successive values of T .

$$\frac{S_a}{g} = 2.5\eta(1.25A) \left(\frac{Q}{R}\right) \left(\frac{T_2}{T}\right)^{\frac{2}{3}} \quad T_2 \leq T \leq 3.0s \quad (1)$$

where: S_a - represents the spectral acceleration; g - represents the gravity acceleration; A - represents the coefficient of zone acceleration ($A = 0.30$); The quality factor "Q" of the structure defined by the Algerian code RPA 2003 depends on the redundancy in the plan, the regularity in the plan, and the elevation. The quality control and material execution in this scenario are for the building group 1B, where $Q = 1.30$; R - represents the coefficient of behaviour: $R = 2$; In this study, we considered URM existing structures to be the lowest class in the masonry category when $R = 2$; T_2 - represents the upper limit of the period defining the horizontal spectral acceleration branch for the considered geologic and geotechnical soil ($T_2 = 0.40s$) and damping correction factor η , given according by the formula Eq. (2):

$$\eta = \sqrt{7/(2 + \xi)} \geq 0,7 \quad (2)$$

$$\eta = \sqrt{7/(2 + 10)} = 0.76 \geq 0,7$$

where: ξ is the proportion of crucial damping based on the constituent material, structural type, and relevance of fillings.

Table 8. Values relating to the elastic response spectrum. Source: RPA 2003

A	η	ξ	R	T1	T2	Q
0.30	0.764	10	2	0.15	0.40	1.30

with: **A** - Rate of acceleration within the zone; **η** - damping correction factor; **ξ** - percentage of critical damping; **R** - ratio of structural behaviour; **T1** and **T2** - characteristic period associated with type of site; **Q** - quality factor.

The following spectrum graph is the outcome of four factors: A (area amplification coefficient), D (dynamic amplification factor), Q (quality factor), and R. (behaviour coefficient). According to the RPA2003 code (Fig. 17), it indicates the connection between S_a/g and the period T (s).

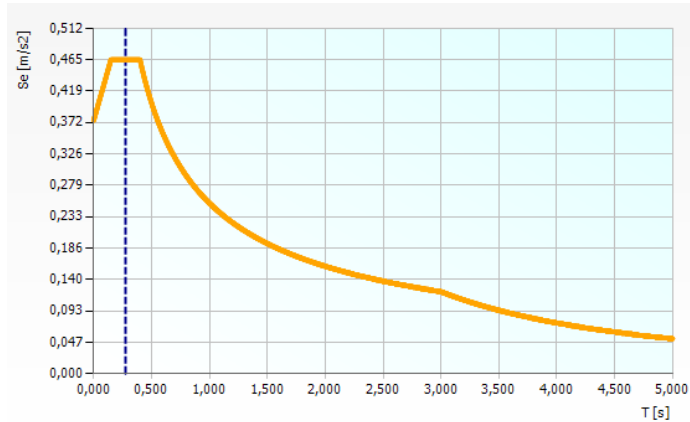
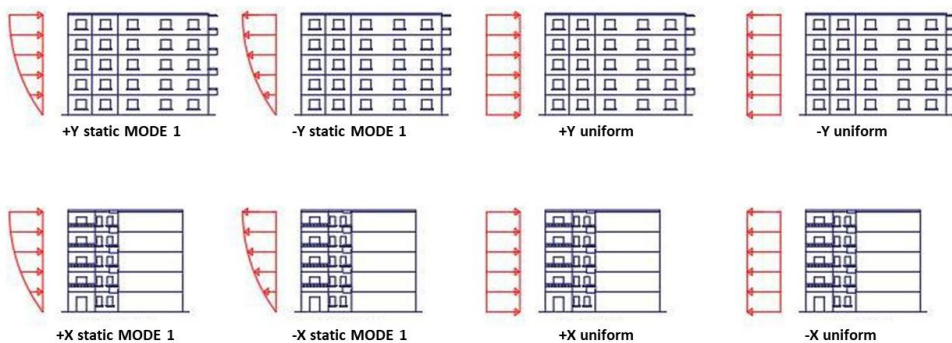


Fig. 17. RPA 2003 Response Spectrum for the Site of El feth high school

Non-Linear Static “Pushover” Analysis:

According to *S. Lagomarsino and S. Cattari* [34] in pushover analysis, the structure will be load with a proper distribution of lateral loads that are gradually increased with the aim of “pushing” the structure into the non-linear field. Two load patterns are taken into consideration, first mode shape distribution based on the fundamental mode shape of the structure, and uniform load distribution to all stories as recommended by different authors for the N-2 and 3muri approach [34, 35]. The load shapes are proportional to mass; The principle consists in subjecting the structure to monotonic loading until it collapses which gives us a force



displacement curve (capacity curve) which represents the general behaviour of the structure [26].

Fig. 18. Load patterns and different cases of pushover analysis, source: Hysenlliu [37]

Once the structure is modelled, “Pushover” analysis can be carried out. To model seismic action, response spectrum data, in our case, calculated in accordance with the Algerian seismic code (RPA 99/2003) [23], is inserted. After introducing the data, structural analysis can be carried out; the Italian standard NTC 2018 [33] anticipates 24 types of analysis, that differ

between the directions x and y (positive and negative in both directions) as well as the loading mode (static and uniform), while taking into account eccentricity.

Results and discussion

Preliminary Modal Analysis

El Feth High School's seismic vulnerability was first carried out by applying a preliminary modal analysis to assess the dynamic behaviour of the structure and the participation of potential damage modes. This analysis is useful to verify the consistency of the assumptions made in terms of material parameters and connections between the different structural systems.

It is worth noting that the current Algerian legislation RPA 2003 [23] defines a mass participation limit of 90% in both directions X and Y in the case of existing and new buildings. The application of linear dynamic analysis in the Italian [33] and European Codes 8 [38] requires considering numerous modes that activate at least 85% of the participating mass.

The results of the modal analysis's first 28 vibration modes are displayed in (Table 9). The participating masses obtained in the X and Y directions reached 90.04 and 92.57 respectively. By observing the results, we notice that the 2nd, 5th, 7th, 11th and 14th modes of vibration are translational along the X axis with periods of 0.40, 0.37, 0.36, 0.28 and 0.27s respectively, whereas those of the 4th, 6th, 8th, 9th and 18th modes of vibration are translational along the Y axis with periods of 0.38, 0.36, 0.36, 0.35, 0.31 and 0.25s respectively. It should be noted that the participating masses along the Z axis are minimal and negligible. Also, it should be remembered that the other modes beyond the 28th vibration mode are translational along the X and Y axes with minimal participating masses that can be neglected.

It should be noted that these results do not reflect the actual behaviour of the construction in its entirety, as masonry constructions involve many unstable parameters, such as the nature and quality of the material as well as the regularity of the building's plan and façade [14].

Table 9. Results of the modal analysis for the first 12 modes (natural period—T, mass x—mx, participating mass along x—Mx, mass y—my, participating mass along y—My, mass z—mz, participating mass along z—Mz)

Mode	T [s]	mx [kg]	Mx [%]	my [kg]	My [%]	mz [kg]	Mz [%]
1	0,42496	17.633,375	0,19	294.621,961	3,16	15,371	0
2	0,40952	2.170.054,319	23,31	56.157,071	0,6	0,13	0
3	0,40446	10.158,792	0,11	219.804,639	2,36	47,323	0
4	0,38822	528.639,620	5,68	834.004,099	8,96	1.136,097	0,01
5	0,37851	822.076,629	8,83	204.705,529	2,2	21,709	0
6	0,36668	494.446,709	5,31	2.452.008,382	26,33	434,411	0
7	0,36099	898.913,946	9,65	329.402,418	3,54	58,097	0
8	0,35387	52.982,621	0,57	692.375,319	7,44	16,09	0
9	0,31418	1.120,279	0,01	562.670,361	6,04	96,203	0
10	0,29781	23.073,919	0,25	4.169,637	0,04	36,309	0
11	0,28895	1.123.722,066	12,07	26,857	0	29,596	0
12	0,28645	2.731,388	0,03	276.022,836	2,96	197,38	0
13	0,28258	133.419,171	1,43	130.533,239	1,4	746,71	0,01
14	0,27284	1.498.992,166	16,1	96,24	0	120,128	0
15	0,27118	393.517,343	4,23	206.033,094	2,21	7,197	0
16	0,26677	28.005,794	0,3	33.513,126	0,36	1,307	0
17	0,26294	28.988,204	0,31	18.269,567	0,2	54,145	0
18	0,25788	429,648	0	1.314.380,655	14,12	211,676	0
19	0,24878	7.977,590	0,09	373.942,139	4,02	39,271	0
20	0,23304	30.671,778	0,33	104.027,265	1,12	17,251	0
21	0,23053	54.740,628	0,59	117.493,777	1,26	253,098	0
22	0,22487	19.458,745	0,21	1.789,756	0,02	265,317	0

23	0,22367	57,19	0	108,891	0	561,158	0,01
24	0,21868	0,075	0	34.297,383	0,37	10,729	0
25	0,21386	13.467,159	0,14	123.143,646	1,32	6,414	0
26	0,21124	9.179,929	0,1	1,075	0	303,226	0
27	0,2088	7.273,976	0,08	39.331,427	0,42	182,344	0
28	0,20658	11.045,812	0,12	11.507,961	0,12	325,628	0
Σ			90,04		90,57		

*The numbers highlighted with fluorescent yellow display the most significant participating masses.

Pushover analyses results

After carrying out the Pushover analysis, the analysis procedure is generated automatically by the program. The analysis of the pushover results in the 3muri software is plotted by the force-displacement curve for each X and Y direction from the 12 curves, the horizontal displacement of the control node (placed at the highest point of the structure; (Fig. 12). The worst-case scenario (the case of least energy dissipation) is chosen as the representative capacity curve in this direction. The curve is then bi-linearised according to the N-2 procedure [39] (Figs. 19 and 20).

In Figures 16 and 17 the capacity curve along the +X and -Y axis respectively represent the two most significant and unfavorable cases in our analysis, the ultimate displacement (D_u) as well as the bilinear curve is demonstrated.

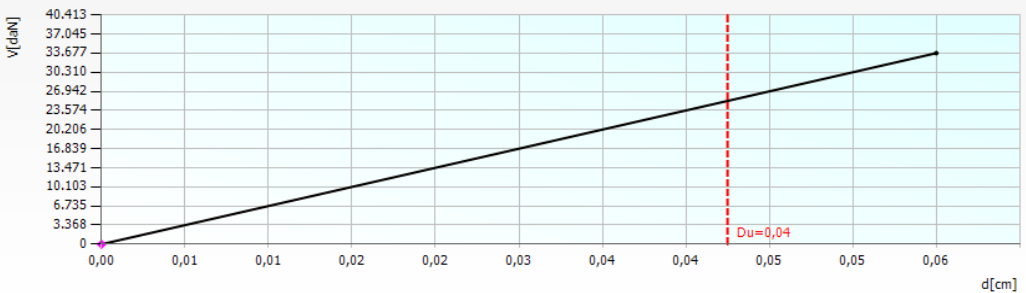


Fig. 19. Capacity curves, corresponding equivalent bilinear curves, and maximum available displacement D_u . Pushover in direction +X

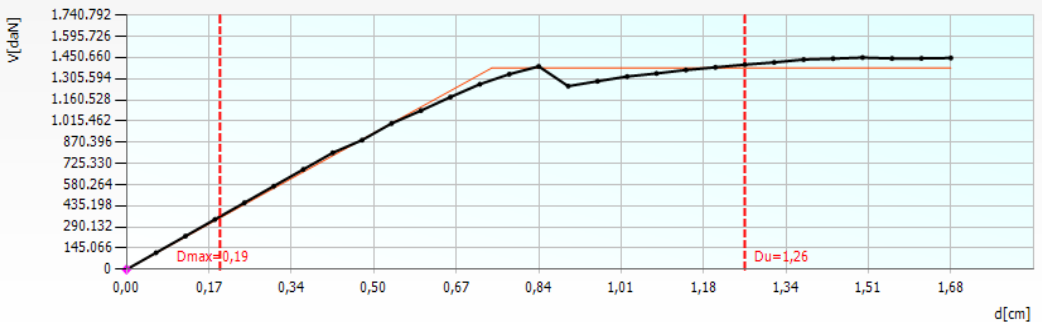


Fig. 20. Capacity curves, corresponding equivalent bilinear curves, and maximum available displacement D_u . Pushover in direction -Y

Figures 21 and 22 illustrate a sample of the most significant walls for analysing the “In-plan” damage of the structure. Taking into account the building's area of coverage, which is 68 m long and 60 m wide, along with the symmetry on the X and Y axes, therefore, a sample of the

most significant walls for analysing the “in-plan” damage of the structure has been chosen. The walls in both diagrams are the same in order to compare the structure's behaviour in the two directions of the analysis.

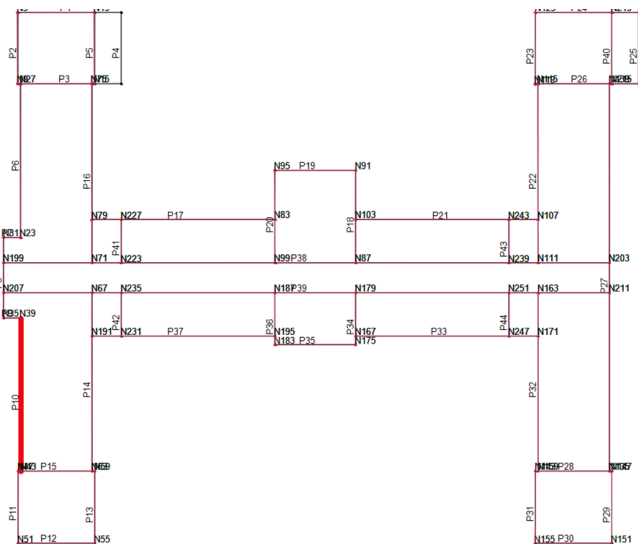


Fig. 21. Designation of walls by 3muri software

The capacity curve shown in Figure 16 along the +X axis demonstrates that the maximum displacement (D_{max}) has exceeded the ultimate displacement (D_u), so we have $D_{max} = 0.39 \text{ cm} > D_u = 0.04 \text{ cm}$ with D_u being in the elastic sequence of the curve.

Figure 19 shows the damage to the main walls of the building, due to the rigidity of the building in the +X direction, the walls did not suffer any significant damage, although there was some bending damage to the spandrels and a little less to the piers, but the majority of the structure did not suffer any apparent damage.

The capacity curve in Figure 20 indicates that the maximum displacement (D_{max}) of the structure did not reach or exceed the ultimate displacement (D_u) due to the elasticity of the structure in the -Y direction, because $D_{max} = 0.19\text{cm} > D_u = 1.26\text{cm}$, however, the walls were severely damaged. Figure 22 shows that the walls (P1 and P32) were only damaged by bending for the "spandrels" and "piers". However, there were bending failures of the walls (P11, P10, P16 and P6), cracks and shear failures occurred on the "piers" of the walls (P8, P16, P6 and P22). The walls (P11 and P16) show the presence of some failures during the elastic phase in the "piers" part.

Comparing figures 22 and 23, it can be seen that the same walls present in the two figures had totally different behaviours and damages, and therefore it can be supposed that the pushover analysis along the -Y direction is the most vulnerable.

The interpretation of the results of the pushover analysis, carried out in addition to the global behaviour of the structure, shows:

- That the thrust along the -Y axis of the central block (Fig. 5) caused a rotation of the two blocks (A and B), which brings us back to our primary deduction in (section 2.1),
- The "H" is a shape that does not satisfy the standards of the current anti-seismic design, especially with the absence of seismic joints.

It is necessary to specify that this pushover analysis cannot identify the out-of-plan behaviour of the structure [14], but only the in-plan behaviour is taken into account.



Fig. 22. Damaged walls after pushover analysis in direction +X

Recommendations of the structure reinforcement:

Several methods and techniques for reinforcing a masonry structure can be found in the literature. In this article we will just give some general solutions that can be studied further in other research in order to reduce the vulnerability of the school in case of future structural rehabilitation.

It should be noted that the recommendations proposed below to improve the behaviour of El Feth High School in the event of an earthquake are a global and non-precise response to the results obtained by the non-linear static pushover analysis. In order to verify the

effectiveness of these recommendations, it is important to note that a more in-depth study of the structure, the current state of the structure, and the materials of which it is composed is required in order to make a comparison before and after the structural rehabilitation intervention. Seismic design in the Italian code NTC 2018 [33] and the Algerian code RPA 2003 [23] recommend regularity in plan, which means avoiding shapes with re-entrant corners and recesses in plan, such as the (H) shape.

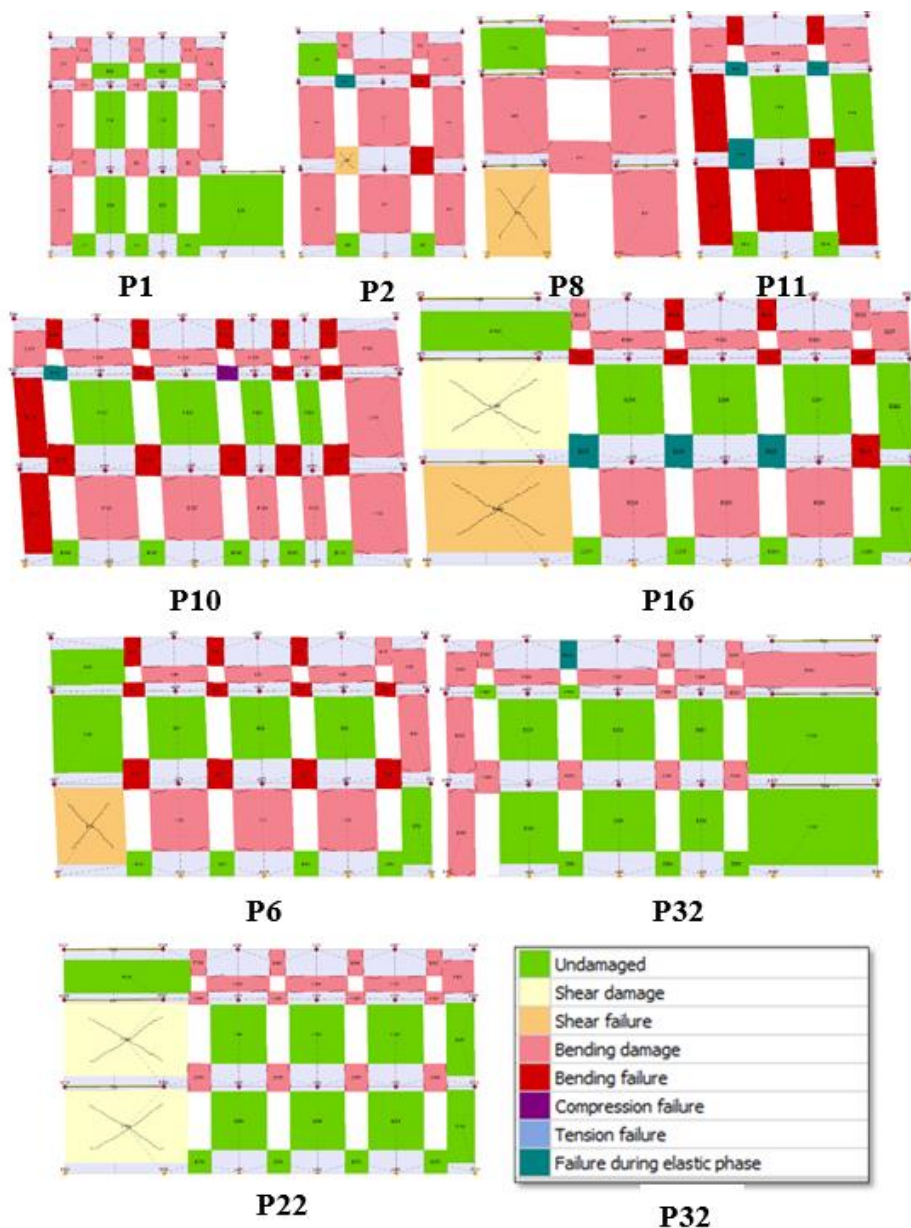


Fig. 23. Damaged walls after pushover analysis in direction -Y

According to *P. Sanketh and B.C.M. Rao* [40] the impact of a re-entrant corner during a seismic event causes two issues:

- Local stress concentration at the re-entrant corner due to wing movement differences
- Torsional movement caused by the building's relative separation of its center of mass and center of stiffness

As previously mentioned, the results obtained after Pushover analysis confirms our original premise that the H form of the building makes it extremely vulnerable in the face of a substantial earthquake (too many projections). And since unreinforced masonry is fragile, it is easily damaged during an earthquake. Furthermore, the existence of a re-entrant corner makes it much more hazardous [41].

To reduce the seismic vulnerability of the structure, we propose to create a seismic joint and transform the structure into three simple blocks (Fig. 25), in order to improve the dynamic behaviour of load-bearing walls.

This process has already been adopted in Algeria during the restoration works after the earthquake in Boumerdes in 2003 of the great mosque of Dellys, whose reconstruction dates back to the French period. One of the major interventions was to separate the minaret from the rest of the mosque with a seismic joint. Therefore, we will apply the same solution (Fig. 24) in the El Feth High School. In fact, we propose to create two seismic joints by detaching the central block from the perpendicular ones.

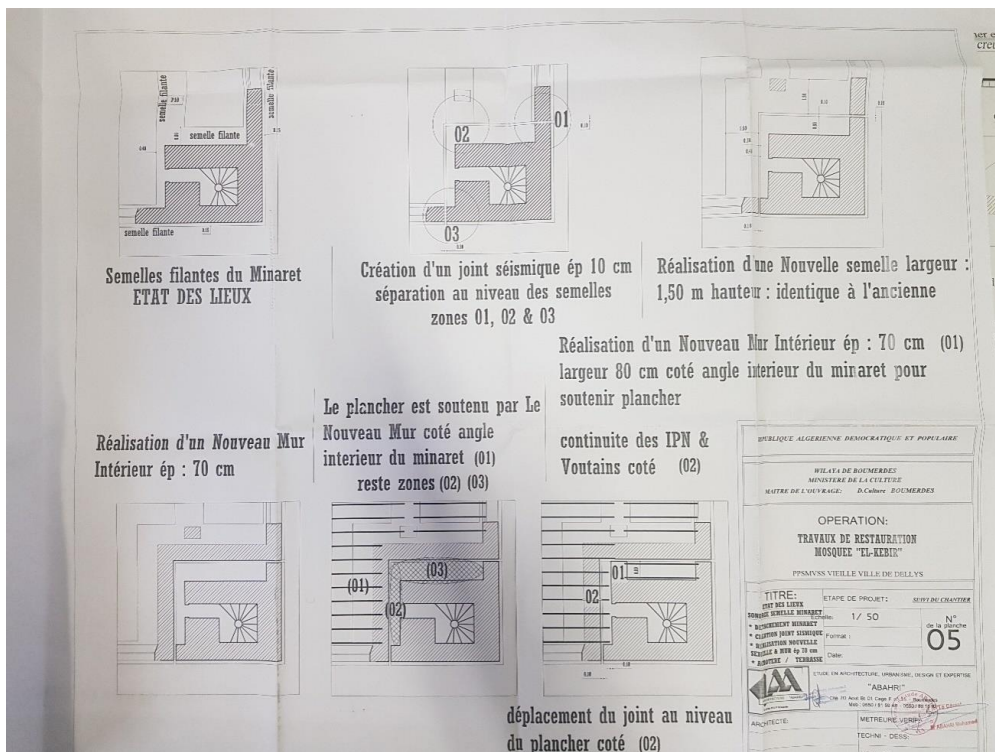


Fig. 24. Drawing depicting the processes used to create the Dellys mosque's seismic joint. Source: Archive of the Technical Service of the Boumerdes Cultural Directorate

Seismic joints as an effective solution:

According to the RPA [23], two neighboring blocks must be separated by seismic joints whose minimum width satisfies the following condition according to (RPA99/2003, Chapter V, Art 5.8):

$$d = 15mm + (\delta_1 + \delta_2)mm \geq 40mm. \tag{3}$$

with: *d* - Seismic joint width; $\delta_1\delta_2$ - the maximum displacements of the two blocks at the top of the lower block, calculated according to (Article 4.4.3 RPA99/V2003) [23].

According to EC8 [38], structures should be simple and regular (in plan and height). If this is not the case, the structure must be dynamically divided into units. As stated in article 2.2.4.1 of EC8:

$$\Delta = \sqrt{d_1^2 + d_2^2} \tag{4}$$

Dimensioning of the seismic joint width:

In order to calculate the minimum width of the seismic joint to prevent the two blocks from colliding during an earthquake we have separated the A-block and the central block (Fig. 5), then a pushover analysis was performed with Temuri on each of the two blocks in order to determine their maximum displacement $\delta_1\delta_2$ of these two neighboring blocks:

$$\delta_1(\text{block A}) = 6.13\text{cm}, \delta_2(\text{block central}) = 2.98\text{cm}$$

According to Rpa 2003 we have:

$$d = 15mm + (61.3 + 29.8) = 105.1mm \geq 40mm$$

This means that the width obtained satisfies the regulations.

According to Eurocode 8 we have:

$$\Delta = \sqrt{(6.13^2 + 2.98^2)} = 6.81\text{cm}$$

In order to ensure optimum safety and ease of execution of the seismic joint we have opted for the width obtained with the Rpa 2003 [23] which is 11cm.

The separation of the three blocks (Fig. 25) will not be an easy manoeuvre. Indeed, this intervention will require a lot of mastery to achieve this

1. All work will take place in the central block.
2. Cut from top to bottom a part of the wall (the part of the wall cut out = the dimension of the joint) of the central block which is 10cm.
3. Once the gap between the three blocks is obtained, a new load-bearing wall must be built on both sides of the central block
4. New load-bearing walls must participate in structural functions.

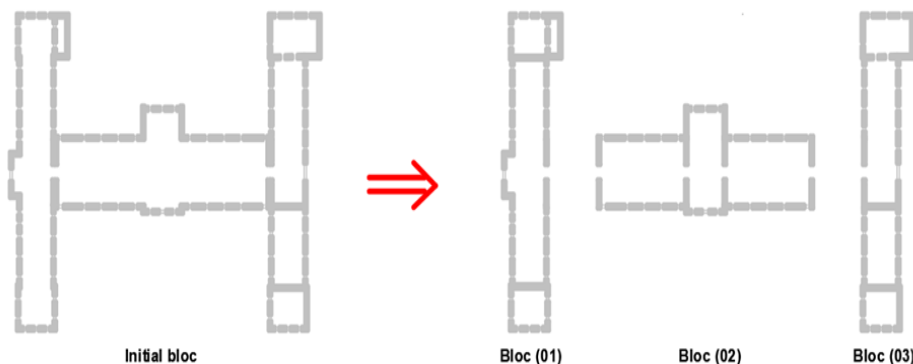


Fig. 25. Illustration of the separation into three blocks. Source: Author

As shown in figure 26, the seismic joint will be executed at the junction between the centre block and blocks A and B. The first step would be to build a new wall (1) with the same physical and mechanical properties as the old one (55cm thick hollow brick). In the northern part of the building, we find a staircase (2) built-in stone that is not participating in the structural behaviour, so it must be demolished and rebuilt after the construction of the wall (1) (Fig. 27).

In order to proceed to the detachment of the two blocks by a seismic joint, with a maximum thickness of 15cm, the wall (1) must be finalized and connected with the IPN profiles of the vaulted floor (3) to make it participate in the support of the vertical loads.

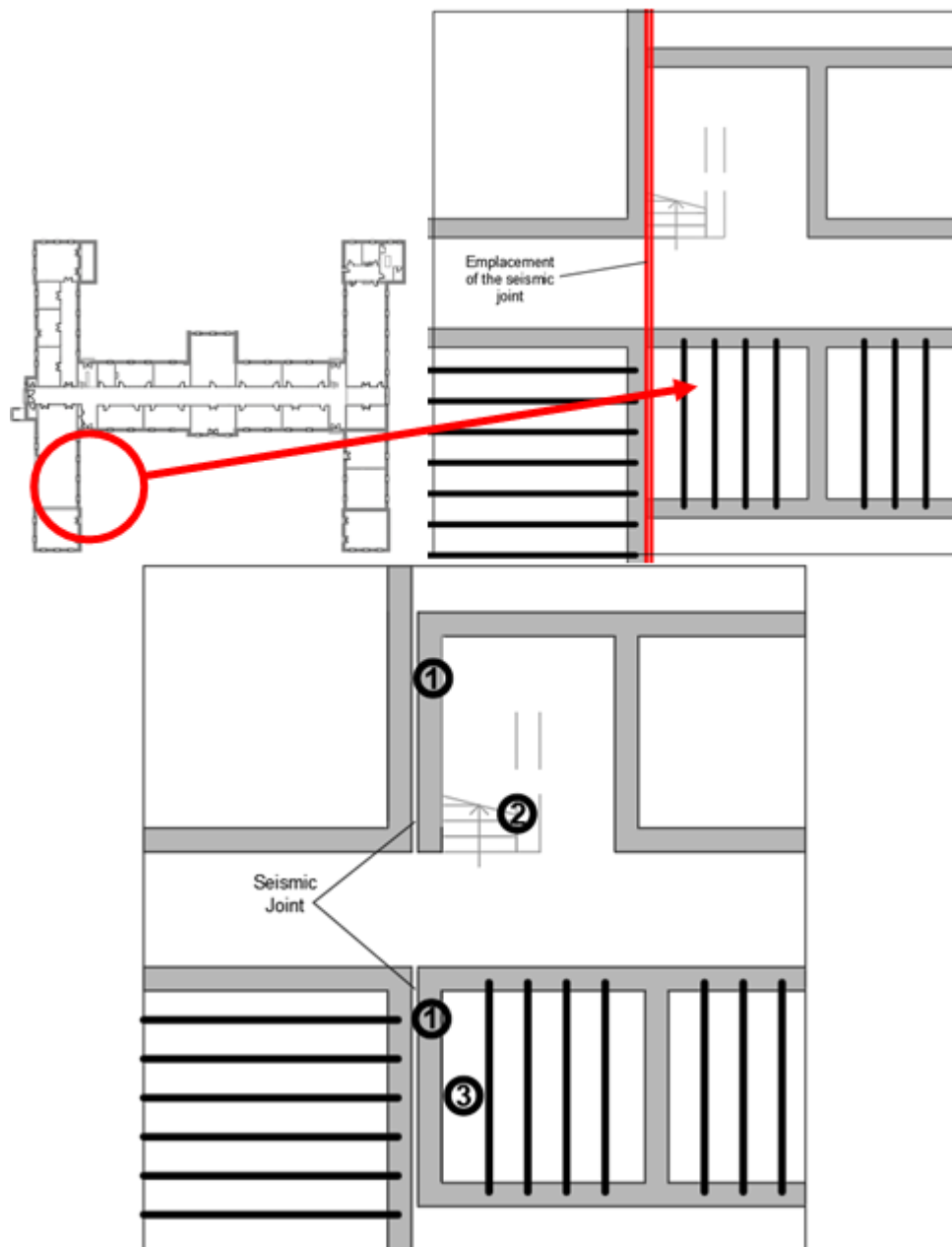


Fig. 26. proposed steps for the integration of the seismic joint between block A and the central block.

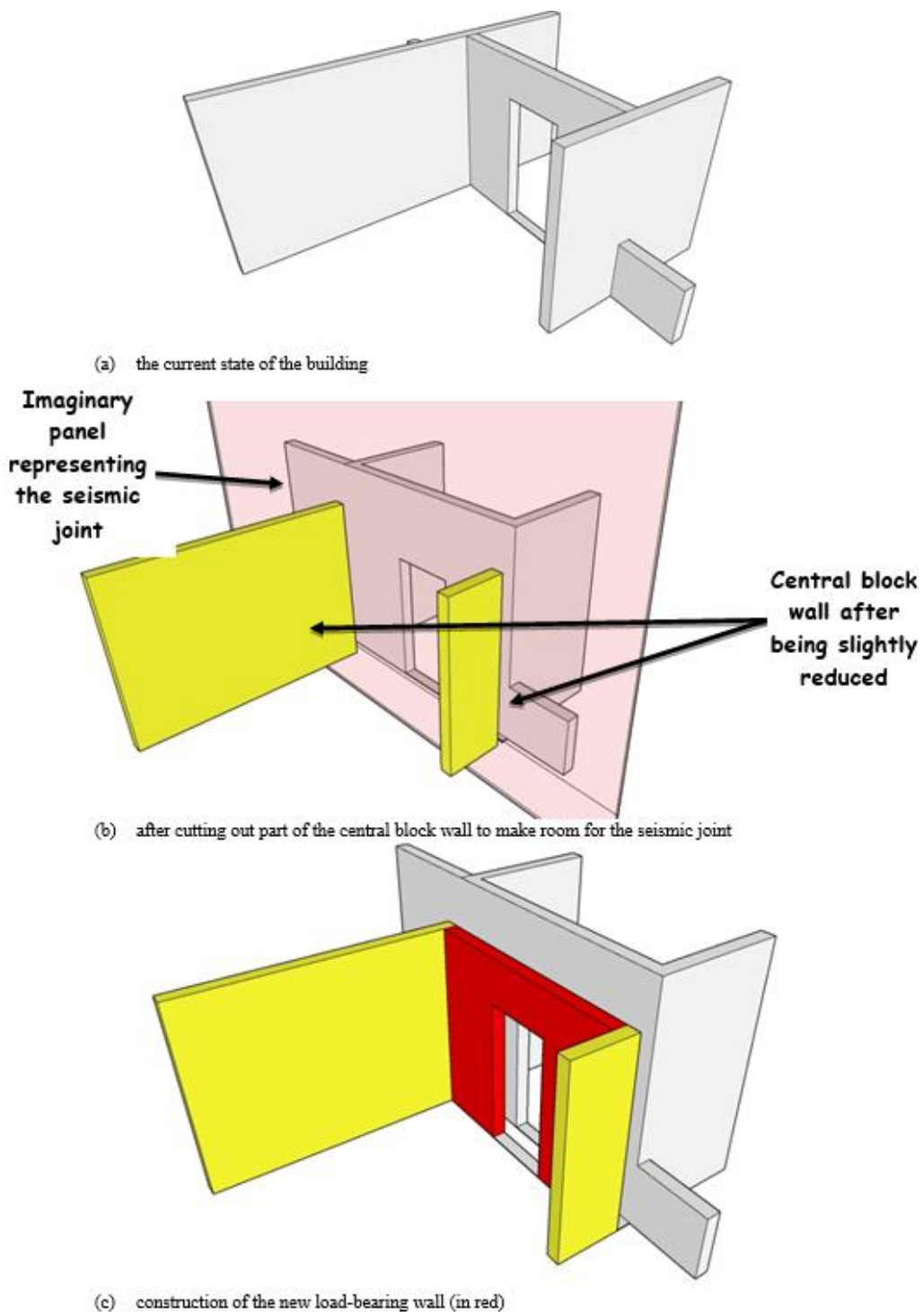


Fig. 27. Sketch of the integration of a seismic joint that will separate O2 blocks.

The TREMURI software does not take into account the three blocks separated at the same time in a single simulation, and given that the analysis has to be carried out one by one, only the central block was taken into account following the significant displacement observed during the first push-over analysis.

The results of the 2nd pushover analysis show that the displacement along the most unfavorable axis, which is "-Y" shown by the 1st analysis, has decreased considerably. Figures 28 and 29 show the comparison between the distortion of the building before and after the addition of the rupture joint.

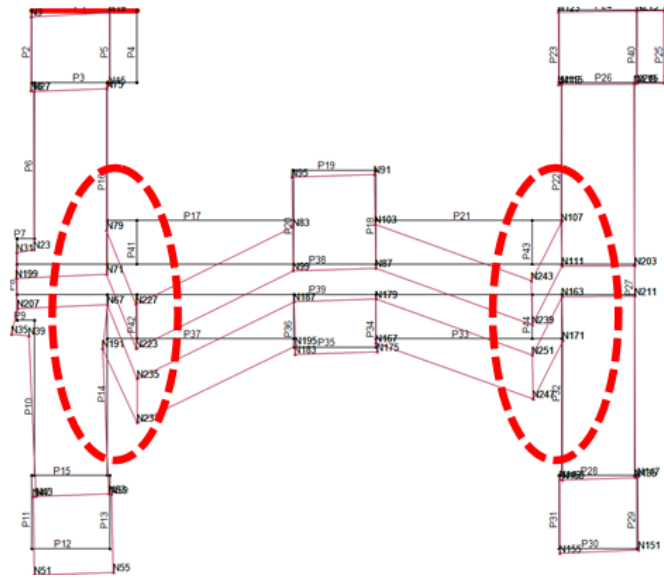


Fig. 28. Distorted plan in direction -Y

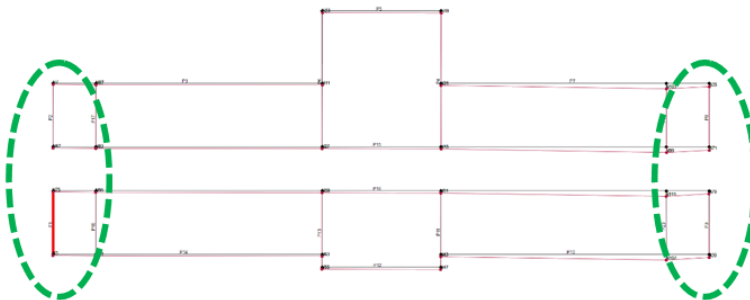


Fig. 29. Distorted plan of the central block in -Y direction

A comparison of the two drawings in the (Fig 28 and 29) shows a clear improvement in the behaviour of the central block at the re-entrant corners with and without a fracture joint, which considerably reduces the deformation and in-plane damage of the walls and eliminates the torsional movement of blocks A and B caused by the distortion of the central block.

To lessen and prevent torsion in the central block, the installation of a seismic joint is the primary focus of our research. At the same time, other damages may occur in the event of an earthquake, such as:

- X-shaped cracks and
- corner detachments
- facade reversals

These will require targeted interventions and reinforcement measures to prevent them.

Conclusions

School buildings in Algeria constitute an important architectural heritage in relation to the architectural style, history, and construction technique. Evaluating the degree of seismic vulnerability of such architecture remains an important challenge in the protection of these constructions and especially of the people who frequently use them (pupils, teachers, staff, etc.).

El Feth high school was symbolically used as a study case from these commonly erected historical architectures and at the same time national educational institutions.

The use of hollow brick with 6 holes, to construct the El Feth High School, was an excellent choice because, 150 years later, the building is still in good condition. Although it is situated in a region of high seismicity, this building material has shown itself to possess good dynamic behaviour, responding favorably to seismic threats. It possesses, therefore, earthquake-resistant properties, which were not taken into consideration at the time of its conception, simply because there were no seismic regulations at that time. Only technical know-how and good quality materials were thought to be sufficient to allow the building to resist temporal conditions (old age ...etc).

In the first observation of the in-situ visit, we deduced a failure in the structure with a flexible floor and an "H" shape with a lack of seismic joint, hence the presence of re-entrant corners in the structure influences the seismic performance of the building. During a seismic event, a re-entrant corner generates stress concentration and torsion problems. The pushover analysis reinforced our preliminary deduction of the vulnerability of the school's structure to an earthquake. This is because the torsion phenomenon was caused by the displacement of the central block along the Y-axis, which led to the rotation along the Z-axis of both blocks A and B.

The seismic joint in the building will undoubtedly be a complex and delicate task to implement, but it is essential for the conservation of this heritage and for the safety of its users.

The installation of a seismic joint will solve our main concern in this research, which is to resolve and avoid the torsion of the central block, which will drag blocks A and B with it. However, due to the lack of information about the corner chaining, the state of connection between floors and vertical walls, as well as the state of the mortar after more than 150 years of existence, it should be taken into account that in the event of an earthquake, probable pathologies of seismic origin on the unreinforced masonry may appear, such as X-shaped cracks and corner detachments or even facade reversals.

The pushover analysis combined modelling with the Tremuri software allowed us to verify the seismic behaviour of the high school structure. The first solutions suggested can be considered to avoid future earthquake damage.

This study may have limitations on the quality of the materials used at the time and their current state due to the lack of available data and the lack of archives concerning this construction. Then the push-over analysis used by this software does not take into account all

aspects of the structure's behaviour (out of plan). Finally, the reaction of the structure after the separation of the three blocks needs to be verified in more detail (post-intervention simulation) in order to define it as a concrete solution for future rehabilitation.

This research is part of our ongoing work assessing the seismic vulnerability of schools constructed with unreinforced masonry. Other types of buildings will be examined in our doctoral thesis and future publications, with the goal of contributing meaningfully to the preservation of this architectural heritage.

Acknowledgments

The authors kindly acknowledge Prof. Giuseppina Uva for her help, orientation. Also Dr. Chaiebdra Belkacem for his help and the Architectural Design office Bouras Djelloul. The authors are also grateful to S.T.A DATA Company for giving us access to their academic version of Tremuri software. They are also grateful to the DGRSDT and Lab ETAP which finance the doctoral training.

References

- [1] F.V. Karantoni, M.L. Papadopoulos, S.J. Pantazopoulou, *Simple Seismic Assessment of Traditional Unreinforced Masonry Buildings*. **International Journal of Architectural Heritage**, **10**(8), 2016, pp. 1055-1077. <https://doi.org/10.1080/15583058.2016.1183062>.
- [2] A. Penna, A. Galasco, M. Tondelli, M. Rota, G. Magenes, *Seismic Vulnerability of Old Italian Railway Stations*, **Structural Analysis of Historical Constructions**, **RILEM Book Series** (Editors: R. Aguilar, D. Torrealva, S. Moreira, M.A. Pando and L.F. Ramos), Springer, Cham., **vol. 18**, 2019. https://doi.org/10.1007/978-3-319-99441-3_132.
- [3] L. Mohammadi, A. Abdessemed Foufa, M. Cheikh Zouaoui, 2021. *Assessment of the seismic behaviour of heritage masonry buildings using numerical modelling: A study of Fernand Pouillon's Totem Tower in Algiers, Algeria*, **Journal of Building Engineering**, **38**, 2021, Article Number: 102183. DOI: <https://doi.org/10.1016/j.jobbe.2021.102183>.
- [4] D. D'Ayala, V. Novelli, *Seismic Vulnerability Assessment: Masonry Structures*, **Encyclopedia of Earthquake Engineering**, (Editors: M. Beer, I.A. Kougoumtzoglou, E. Patelli and S.K. Au), Springer, Berlin, Heidelberg, 2015. https://doi.org/10.1007/978-3-642-35344-4_250
- [5] A. Preciado, A. Orduña, G. Bartoli and H. Budelmann. *Facade seismic failure simulation of an old Cathedral in Colima, Mexico by 3D Limit Analysis and nonlinear Finite Element Method*, **Engineering Failure Analysis**, **49**, 2015, pp. 20-30. <https://doi.org/10.1016/j.engfailanal.2014.12.003>
- [6] J.A. Peláez Montilla, M. Hamdache, C. López Casado, *Seismic hazard in Northern Algeria using spatially smoothed seismicity. Results for peak ground acceleration*, **Tectonophysics**, **372**(1), 2003, pp. 105-119. [https://doi.org/10.1016/S0040-1951\(03\)00234-8](https://doi.org/10.1016/S0040-1951(03)00234-8)
- [7] * * *, **Centre de recherche en astronomie, astrophysique et géophysique (CRAAG)**, https://www.craag.dz/r_sismologique.php [accessed 09, August 2023].
- [8] A. Yelles-Chaouche, C. Aidi, H. Beldjoudi, I. Abacha, A. Chami, O. Boulahia, ... & H. Bendjama, (2022). *The recent seismicity of northern Algeria: the 2006–2020 catalogue*. **Mediterranean Geoscience Reviews**, **4**(4), 407-426.

- [9] D. Stich, C. J. Ammon, & J. Morales, (2003). *Moment tensor solutions for small and moderate earthquakes in the Ibero-Maghreb region*. **Journal of Geophysical Research : Solid Earth**, **2003**, vol. 108, no B3.
- [10] A. Harbi, Amal Sebaï, Yasmina Rouchiche, S. Maouche, F. Ousadou, K. Abbes, Dalila Ait Benamar and Manel Benmedjber. "Reappraisal of the Seismicity of the Southern Edge of the Mitidja Basin (Blida Region, North-Central Algeria)." **Seismological Research Letters**, 88 (2017): 1163-1177. <https://doi.org/10.1785/0220160217>.
- [11] S. Maouche and A. Harbi. *The active faults of the Mitidja basin (North Central Algeria): what does the seismic history of the region tell us? A review*. **Euro-Mediterranean Journal for Environmental Integration**, 3 (2018): 1-11. <https://doi.org/10.1007/s41207-018-0061-1>.
- [12] M. Boukri, M. Farsi, A. Mebarki, M. Belazougui, M. Ait-Belkacem, N. Yousfi, N. Guessoum, Dalila Ait Benamar, M. Naili, N. Mezouar and O. Amellal. *Seismic vulnerability assessment at urban scale: Case of Algerian buildings*. **International Journal of Disaster Risk Reduction** (2018). <https://doi.org/10.1016/J.IJDRR.2018.06.014>.
- [13] * * *, RPA2024, *Document Technique Réglementaire D.T.R. - B.C. 2.48, Règles Parasismiques Algériennes*, **Centre National de Recherche Appliquée en Génie Parasismique**, Alger, 2024.
- [14] K. Amari, A. Abdessemed Foufa, M. Cheikh Zouaoui, G. Uva, *Seismic Vulnerability of Masonry Lighthouses: A Study of the Bengut Lighthouse, Dellys, Boumerdès, Algeria*, **Buildings**, **10**(12), 2020, Article Number: 247. <https://doi.org/10.3390/buildings10120247>.
- [15] A. Abdessemed-Foufa, & D. Benouar (2003). *Damage survey of the old nuclei of the Casbah of Dellys (Algeria) and performance of preventive traditional measures in the wake of the Boumerdes 2003 earthquake*. **European Earthquake Engineering Journal**, 3(10).
- [16] C.E. Chitour, **L'Education et la culture de l'Algérie : des origines à nos jours**, Ed. **ENAG**, 1999, 302p.
- [17] D.J. Vickery, **School Buildings and Natural Disasters**, UNESCO, 1984, 93p.
- [18] * * *, United Nations Office for Disaster Risk Reduction (ONU), *Disaster risk reduction begins at school: 2006-2007*, **World Disaster Reduction Campaign**, 2007, 25p.
- [19] G. Kenny, *Disaster Management and Educational Facilities*, **PEB Exchange, Programme on Educational Building**, n° **09/2002**, Éditions OCDE, Paris, <https://doi.org/10.1787/737054181070>.
- [20] S. Khelifa-Rouaïssia, H. Boulkroune, *The Architecture of the Town Halls of the French Colonial Period in Algeria: The First Half of Nineteenth Century*, **International Journal of Historical and Archaeology**, **21**(2), 2017, pp. 420–432. Special Issue 1. <https://doi.org/10.1007/s10761-016-0352-7>
- [21] J. Park, P. Towashiraporn, J. Craig, & B. Goodno, *Seismic fragility analysis of low-rise unreinforced masonry structures*. **Engineering Structures**, **31**(1), 2009, pp. 125-137. <https://doi.org/10.1016/j.engstruct.2008.07.021>
- [22] Z. Boutaraa, C. Negulescu, A. Arab, O. Sedan, *Buildings Vulnerability Assessment and Damage Seismic Scenarios at Urban Scale: Application to Chlef City (Algeria)*, **KSCE Journal of Civil Engineering**, **22**, 2018, pp. 3948–3960. <https://doi.org/10.1007/s12205-018-0961-2>

- [23] * * *, *RPA Règles Parasismiques Algériennes, Report DTR BC 2–48, Centre National de Recherche Appliquée en Génie Parasismique*, Alger, 2003.
- [24] P. Borie, **Projet d'établissement au Puy d'une manufacture de produits en terre cuite pour le bâtiment**, Hachette Livre, 2018, 54p. (in French).
- [25] É. Lejeune, *Guide du briquetier, du fabricant de tuiles, carreaux, tuyaux et autres produits de terre cuite: Guide du chaudronnier, du plâtrier* [Guide of the brick layer, of the manufacturer of tiles, tiles, pipes and other terra cotta products: Guide of the lime Works, the plasterer]. Librairie du **Dictionnaire des arts et manufactures, 1870**, 668p. <http://ark.bnf.fr/ark:/12148/cb30782268w> (in French)
- [26] A. Gratry, **Description des appareils de maçonnerie les plus remarquables employés dans les constructions en brique**, 1865, Paris. <http://ark.bnf.fr/ark:/12148/cb30536104z> (in French).
- [27] * * *, *Nouvelles de Blida, passé et présent* <http://blida.net/fra/2014/03/30/quelques-reperes-de-blida-les-ecoles/> [accessed August, 9th 2023].
- [28] T. Taguchi, C. Cuadra, *Influence of bond types on brickmasonry strength*, **The 15th World Congress on Advances Instructural Engineering and Mechanics (ASEM 15)**, Korea, 2015.
- [29] M. Mosoarca, I. Onescu, E. Onescu and A. Anastasiadis. *Seismic vulnerability assessment methodology for historic masonry buildings in the near-field areas*. **Engineering Failure Analysis**, 115 (2020): 104662. <https://doi.org/10.1016/j.engfailanal.2020.104662>.
- [30] S. Lagomarsino, et al., *TREMURI program: An equivalent frame model for the nonlinear seismic analysis of masonry buildings*, **Engineering Structures**, **56**, 2013. pp. 1787-1799. <https://doi.org/10.1016/j.engstruct.2013.08.002>.
- [31] L. Gambarotta, S. Lagomarsino, *Damage models for the seismic response of brick masonry shear walls. part i: the mortar joint model and its applications*, **Earthquake Engineering & Structural Dynamics**, **26**(4), 1997, pp. 423-439. [https://doi.org/10.1002/\(SICI\)1096-9845\(199704\)26:4<423::AID-EQE650>3.0.CO;2-%23](https://doi.org/10.1002/(SICI)1096-9845(199704)26:4<423::AID-EQE650>3.0.CO;2-%23)
- [32] A. Abdessmed-Foufa, A. Misseri, G.L. Rovero, *Effects of the Boumerdès earthquake of May 21st, 2003 on the Great Mosque of Dellys (Algeria) and Solutions of the Restoration Project*. In **Proceedings of the Vienna Congress on Recent Advances in Earthquake Engineering and Structural Dynamics**, Vienna, Austria, 28–30 August 2013, Wien, **Paper No. 108**
- [33] * * *, MIT (2018) NTC (2018): D.M. del Ministero delle Infrastrutture e dei trasporti del 17/01/2018, Aggiornamento delle **Norme Tecniche per le Costruzioni** (in Italian).
- [34] S. Lagomarsino, S. Cattari, *Seismic Performance of Historical Masonry Structures Through Pushover and Nonlinear Dynamic Analyses*, **Perspectives on European Earthquake Engineering and Seismology. Geotechnical**, (Editor: A. Ansal), **Geological and Earthquake Engineering** (Springer, Cham.), **39**, 2015, https://doi.org/10.1007/978-3-319-16964-4_11.
- [35] A. Galasco, S. Lagomarsino, A. Penna, *On the use of pushover analysis for existing masonry buildings*, **Proceedings of the 13th European Conference on Earthquake Engineering, Geneva (CH)**, 3–8 September 2006, ID 1080.
- [36] Fajfar, P.; Marušić, D.; Perus, I. *Torsional effects in the pushover-based seismic analysis of buildings*, **Journal of Earthquake Engineering**, **9**, 2005, pp. 831–854.
- [37] M. Hysenlliu, M. (2020) *Vulnerability assessment of current masonry building stock in albania*, **PhD Thesis**, Epoka University, 426p <http://dspace.epoka.edu.al/handle/1/2121>.

- [38] * * *, **European Standard EN 1998-1-2004: Eurocode 8: Design of structures for earthquake Resistance**, 'Comite' Europe`en de Normalisation, Bruxelles, 2004.
- [39] P. Fajfar, P. Gašperšič, *The n2 method for the seismic damage analysis of rc buildings*. **Earthquake Engineering & Structural Dynamics**, **25**, 1996, pp. 31-46. [https://doi.org/10.1002/\(SICD\)1096-9845\(199601\)25:1<31::AID-EQE534>3.0.CO;2-V](https://doi.org/10.1002/(SICD)1096-9845(199601)25:1<31::AID-EQE534>3.0.CO;2-V).
- [40] P. Sanketh, B.C.M. Rao, *Effect of symmetrical floor plan shapes with re-entrant corners on seismic behavior of RC buildings*, **i-Manager's Journal on Structural Engineering**, **4**(2), 2015, Article Number: 15.
- [41] A. Aşıkoğlu, G. Vasconcelos, P.B. Lourenço, *Overview on the Nonlinear Static Procedures and Performance-Based Approach on Modern Unreinforced Masonry Buildings with Structural Irregularity*, **Buildings**, **11**(4), 2021, Article Number: 147. <https://doi.org/10.3390/buildings11040147>.
-

Received: July 27, 2023

Accepted: July 4, 2024